1-1-2003

Lossy Data Compression for Imaging Interferometer Data using a Wavelet Transform-Based Image Compresion Algorithm

Gregory W. Cantwell

Scott Budge
Utah State University

Gail E. Bingham

Cantwell, Gregory W., Scott E. Budge, and Gail E. Bingham. 2003. "Lossy Data Compression for Imaging Interferometer Data Using a Wavelet-Transform-Based Image Compression Algorithm." *Proceedings of SPIE* 5157, 190. doi:10.1117/12.509701.

Lossy data compression for imaging interferometer data using a wavelet transform-based image compression algorithm

Gregory W. Cantwell[a], Scott E. Budge[b], and Gail E. Bingham[a]

[a]Space Dynamics Laboratory, 1695 North Research Park Way, North Logan, UT 84341-1947
[b]Dept. of Electrical and Computer Engineering, Utah State University, Logan, UT 84322-4120

ABSTRACT

Data compression on future space-based imaging interferometers can be used to reduce high telemetry costs, provided the performance is acceptable. This paper investigates lossy data compression of imaging interferometer datacubes using a wavelet transform-based compression algorithm, the Set Partitioning in Hierarchical Trees (SPIHT) image compression algorithm. Compression is performed on individual frames of the interferometer datacubes. Simulated datacubes from the Geosynchronous Imaging Fourier Transform Spectrometer (GIFTS) are modified to produce new complex GIFTS datacubes used to perform the experiments. Separate programs are written for the encoder and decoder in C++. The encoder and decoder are simulated to the bit-level, meaning they simulate the exact bit streams that would be generated by hardware implementations. All compression ratios reported are based on the actual file size of the encoded data. The simulations indicate very high performance of the algorithm in the interferogram domain, with average errors of less than one least significant bit (LSB) for the GIFTS long-wave band and just over one LSB for the GIFTS short/mid-wave band at compression ratios as high as 13.7:1 and 15.4:1, respectively. At the same compression ratios, errors in the spectral radiance domain are comparable to the simulated instrument noise and RMS temperature profile retrieval errors of less than 1 K are achieved using a University of Wisconsin-Madison prototype retrieval algorithm.

Keywords: data compression, GIFTS, imaging interferometer, SPIHT

1. INTRODUCTION

Data compression on future space-based imaging interferometers can be used to reduce high telemetry costs, provided the performance is acceptable. An example of a space-based imaging interferometer is the Geosynchronous Imaging Fourier Transform Spectrometer (GIFTS)[1, 2] currently being designed by a team consisting of members from NASA Langley Research Center (LaRC) in Hampton, Virginia; Space Dynamics Laboratory (SDL) in Logan, Utah; and the University of Wisconsin (UW) in Madison, Wisconsin. GIFTS is part of NASA's New Millennium Program Earth Observing 3 (NMP EO-3) mission.

One of the purposes of the GIFTS mission is to serve as a forerunner or prototype for the next generation of geosynchronous operational satellites.[2] The infrared spectra measured by GIFTS will be used to calculate vertical profiles of temperature and water vapor over a 512 × 512 km area (with a spatial resolution of 4 × 4 km). By tracing the movement of water vapor over time GIFTS will also allow for the measurement of winds.

The data compression algorithm presented in this paper has application to future space-based imaging Fourier transform spectrometers (FTS) where the type and amount of data will be comparable to GIFTS. In this paper simulated GIFTS datacubes are used for purposes of testing the algorithm. Compression is performed on the raw interferometer data. Compressing the data in the interferogram domain greatly reduces on-board processing and storage requirements. Since the algorithm presented here operates on individual frames on the GIFTS datacubes, it requires on-board storage for only two frames of data, one for each GIFTS band. The performance of the algorithm at several compression rates is measured in the interferogram domain, spectral radiance domain and in the retrieved temperature and water vapor domains.

Further author information: (Send correspondence to Gregory W. Cantwell)
Gregory W. Cantwell: E-mail: greg.cantwell@sdl.usu.edu, Telephone: (435) 797-4668

Proceedings of SPIE Vol. 5157 Optical Spectroscopic Techniques and Instrumentation for Atmospheric and Space Research V, edited by Allen M. Larar, Joseph A. Shaw, Zhaobo Sun (SPIE, Bellingham, WA, 2003) · 0277-786X/03/$15.00

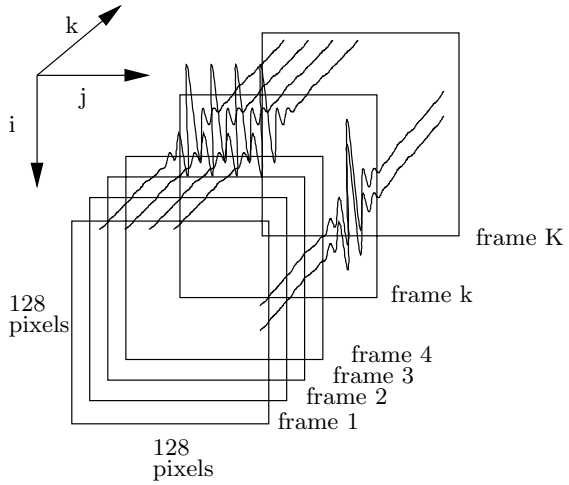

Figure 1. Cube geometry.

1.1. Overview of the GIFTS instrument

At the heart of the GIFTS instrument is an imaging Michelson interferometer. Radiation passing through the interferometer in GIFTS is focused on two separate focal plane arrays (FPAs) of 128 × 128 detectors each.[3] One of the FPAs in GIFTS will detect radiation in the 4.44–6.06 μm IR band and the other in the 8.85–14.60 μm IR band. We will refer to the 4.44–6.06 μm band as the short/mid-wave IR band (SMWIR) and the 8.85–14.60 μm band as the long-wave IR band (LWIR). The bands above can be re-expressed in terms of wavenumbers as 1650–2250 cm^{-1} (SMWIR) and 685–1130 cm^{-1} (LWIR).

The AC component of the signal measured by each detector as a function of the optical path difference (OPD) between the two branches in the interferometer is an interferogram. It can be shown that the Fourier transform of the (ideal) interferogram gives the spectral distribution of radiation entering the interferometer.[4]

After on-board processing which includes co-adding samples, bandpass digital filtering, and decimation, the raw data can be visualized as two 3-D datacubes with dimensions 128 × 128 × 2048 samples (LWIR) and 128 × 128 × 4096 samples (SMWIR). Each sample is a 16-bit 2's complement number. Two of the dimensions in the datacubes are spatial (128 × 128) and the third is the OPD or interferogram dimension. Since the coefficients of the bandpass digital filter are complex, the interferograms are 1024-point and 2048-point complex signals for the LWIR and SMWIR bands, respectively. The cube geometry is shown in Fig. 1. Each detector, or pixel, in the 128×128 detector arrays produces an interferogram. The k^{th} "frame" is defined as the 128×128 image composed of the k^{th} sample (either a real or imaginary sample) from all interferograms. Frame 1 in Fig. 1 is a frame of the real samples from the first complex point of the interferograms, frame 2 is a frame of the imaginary samples from the first complex sample, etc. Throughout the paper the indices i, j, and k are generally used to index samples of the cube; i, j locates a pixel or spatial position, and k indexes the k^{th} sample of the interferogram.

Pixel-to-pixel FPA non-uniformities present a problem for an algorithm which compresses the frames of an imaging FTS datacube. In order to reduce the effects of pixel-to-pixel non-uniformities, the GIFTS on-board processing includes a bad pixel replacement in which samples from a pixel with unusually high or low responsivity, extremely high noise, or a high degree of non-linearity are replaced by samples from a nearby good pixel. At the time this research was conducted the on-board processing also included a first order non-uniformity correction (NUC) in order to "flat field" the data.

The total data rate of the raw data from both FPAs after the filter/decimation stage of on-board processing is 134.2 megabits per second (Mbps). For a target downlink bit rate of 10 megabits-per-second (Mbps), which is in the range of modest telemetry systems on operational and research satellites,[5] this implies a target compression ratio of approximately 13.4:1. The lossy compression algorithm in this paper is tested at compression ratios in the range from 8:1–16:1. These data rates serve to show what may be expected for future space-born imaging FTS sensors with applications similar to GIFTS.

2. SYNTHETIC COMPLEX GIFTS DATACUBES

For the experiments in this paper, synthetic GIFTS datacubes generated by the University of Wisconsin-Madison (UW)[5–7] are modified to produce new complex GIFTS datacubes. The assumption is made that the spectrum of a complex interferogram is essentially the positive (or negative) frequency portion of the spectrum of a real interferogram. Therefore, the original UW GIFTS datacubes are transformed to the spectral domain, the first bin is set to zero (to simulate a bandpass filter), and then the positive frequency half of the spectrum is transformed back into the interferogram domain. This essentially simulates an ideal complex digital bandpass filter.

Since the FTS simulator did not attempt to simulate the A/D converter, it is necessary to quantize the data to 16-bit 2's complement values. Also, the on-board NUC used to flat field the data is assumed to be perfect. This is a critical assumption since it effectively removes any pixel-to-pixel non uniformities caused by an imperfect focal plane array. Performing the on-board NUC can be considered a pre-processing step of the algorithm.

New complex datacubes are generated from UW Cubes 2 and 5, as well as the original UW blackbody cubes at temperatures of 300 K, 265 K, and 2.7 K. We will refer to the new cubes as Complex Cubes 2 and 5 and Complex Blackbody Cubes at their respective temperatures. Complex Cubes 2 and 5 are used for the simulations in this paper. The Complex Blackbody Cubes are used in the calibration equation to convert interferograms to spectral radiance measurements.

Fig. 2(a) shows a sample quantized complex interferogram from pixel (64,64) of LWIR Complex Cube 2. Fig. 2(b) shows a close up of the first resonance due to CO_2 absorption.[5]

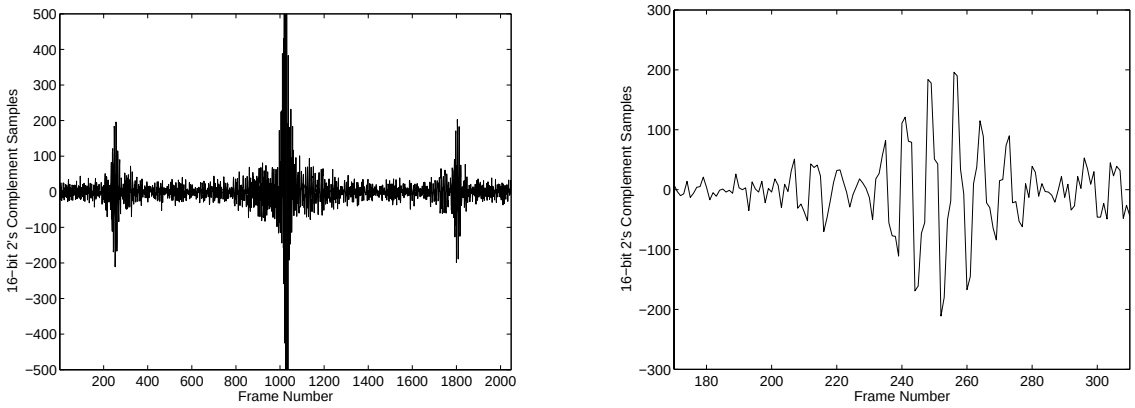

(a) Full length, Y-axis zoomed.

(b) Near first resonance due to CO_2 absorption.

Figure 2. Interferogram from pixel (64,64) of LWIR Complex Cube 2.

Fig. 3 shows a real frame near zero-path-difference (ZPD) in LWIR Complex Cube 2. In this near-ZPD frame, the pixels with large values correspond to warmer locations in the scene while the pixels with small values correspond to colder locations, much of which is due to the presence of clouds.

In an imaging interferometer, some of the beams emerging from the source travel through the interferometer at non-zero angles with respect to the optical axis. Consequently, if all detectors are sampled at the same time, each detector will have its own unique OPD sampling interval dependent on the angle made by the respective beams with the optical axis.[8] This adds extra complexity to the data. Fig. 4 shows two consecutive frames, a real and imaginary frame, respectively, from LWIR Complex Cube 2 in the first CO_2 resonance region. The "rings" observed in these images are evidence of the OPD sample interval differences for off-axis detectors.

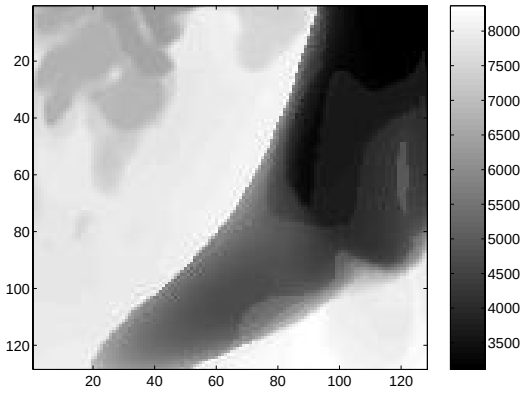

(a) Frame 1025.

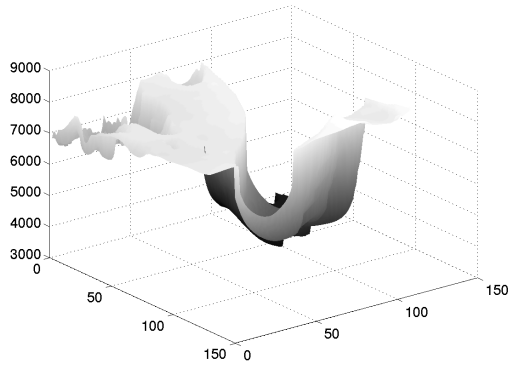

(b) Frame 1025 contour.

Figure 3. LWIR Complex Cube 2 frame 1025.

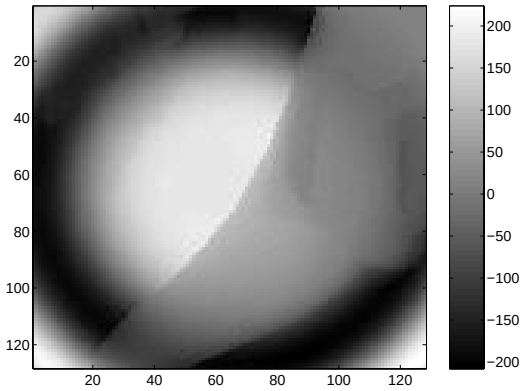

(a) Frame 249.

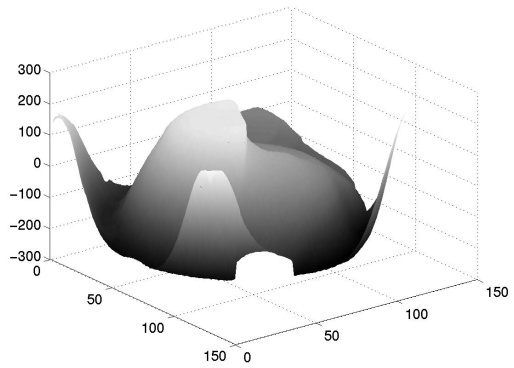

(b) Frame 249 contour.

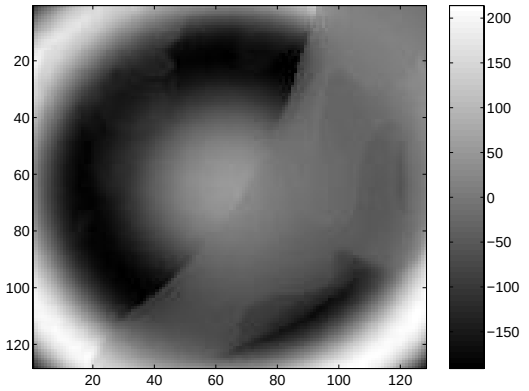

(c) Frame 250.

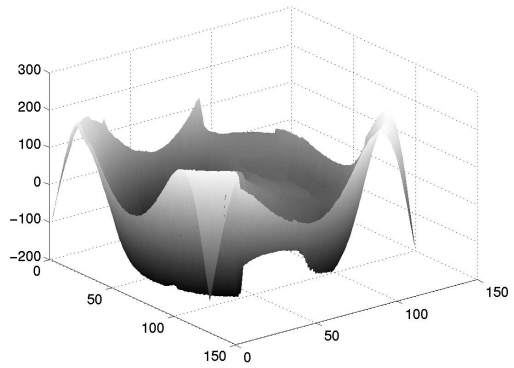

(d) Frame 250 contour.

Figure 4. Two consecutive frames from LWIR Complex Cube 2.

3. GIFTS-SPIHT ALGORITHM

The algorithm investigated in this paper is an application of the Set Partitioning in Hierarchical Trees (SPIHT)[9] image compression algorithm to the GIFTS datacubes. The GIFTS-SPIHT algorithm operates on individual frames of the Complex GIFTS datacubes. The SPIHT algorithm is a very efficient method of coding the wavelet transform coefficients of an image and produces and embedded bitstream. It is currently one of the premier image compression algorithms and serves as a benchmark for very high performance image compression algorithms applied to the frames of imaging FTS raw datacubes.

3.1. GIFTS-SPIHT encoder

The basic algorithm for encoding a frame is as follows.

1. Wavelet transform the frame.
2. Quantize the wavelet transform coefficients.
3. Encode the quantized coefficients with *Algorithm II* in Said and Pearlman's paper[9] using $b_{alloc}(k)$ bits.

These steps are applied repeatedly for each frame in the cube.

The 2-D floating-point wavelet transform with coefficients given in Table II of Antonini et al.[10] is used. This transform is commonly referred to as the 9/7 transform. The wavelet transform is computed with 4 levels of decomposition. The boundaries are handled by implementing each of the intermediate 1-D transforms as a symmetric extension transform.[11]

3.2. GIFTS-SPIHT Decoder

The basic algorithm for decoding a frame is as follows.

1. Decode the quantized coefficients with the decoding version of *Algorithm II* in Said and Pearlman's paper[9] using $b_{alloc}(k)$ bits.
2. Dequantize the wavelet transform coefficients.
3. Perform the inverse wavelet transform on the coefficients.

These steps are applied repeatedly for each frame in the cube. The same $b_{alloc}(k)$ used in the encoder is used as an input to the decoder when decoding the coefficients in step 1) above.

3.3. Bit allocation

A key input parameter to the GIFTS-SPIHT encoder and decoder is $b_{alloc}(k)$, which is a specification of the number of bits to be used in coding/decoding each frame k. We will refer to this parameter as the "bit allocation." The bit allocations used here were initially derived for the original GIFTS cubes based on the assumption that frames having higher entropy should be allocated more bits, and that the number of bits generated per frame by a lossless DPCM encoder[12] is a good indicator of the entropy of the frames. It was also assumed that frames near ZPD, and for LWIR cubes, frames near the first resonance due to CO_2 absorption should be allocated more bits. This assumption is supported by Huang et al.[5] who state that information in these two regions contain most of the temperature profile information content and must be preserved.

In order to preserve the quality of these regions, frames 230–270, 1005–1045, and 1779–1819 for LWIR bit allocations and frames 2029–2069 for SMWIR bit allocations were allocated the same number of bits as were generated by the lossless DPCM encoder. For all other frames, bits were allocated in multiples of 1024 bits by weighting the bits generated by the DPCM encoder. Bit allocations for LWIR and SMWIR Cubes 2 and 5 at nominal target bit rates of 1.0 bpp, 1.5 bpp, and 2.0 bpp are generated. These same bit allocations, although not optimal, are used here for the GIFTS Complex Cubes. It is pointed out that the actual allocations are slightly over the nominal target average bit rates. However, this is not viewed as a problem since the nominal target bit rates are somewhat arbitrarily chosen anyway. Fig. 5 shows a sample bit allocation for LWIR Complex Cube 2.

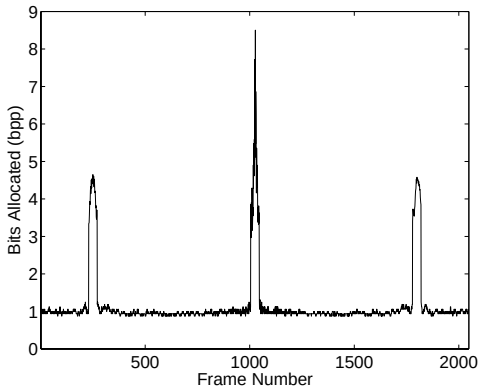

Figure 5. Bit allocation for LWIR Complex Cube 2 at nominal average bit rate of 1.00 bpp.

4. METHODOLOGY

A separate program was written in C++ for both the encoder and decoder. The software encoder simulates the encoder being tested to the bit-level, meaning that it simulates the exact bit-stream that would be generated by a hardware implementation of the encoder. Similarly, the software decoder simulates the decoder under test to the bit-level. For each test, the encoded bits are written to a file as the encoder compresses the data. The file containing encoded data is then read by the decoder, the data is decompressed, and a file containing the decompressed, or decoded, data is written. This provides a complete end-to-end simulation.

All compression rates reported are based on the actual file size of the encoded data. Bit rates reported in bits per pixel (bpp) are calculated as the number of bits in the encoded file divided by the total number of samples in the cube. Compression ratios are calculated as the number of bits in an original cube divided by the number of bits in the encoded file.

In order to evaluate the GIFTS-SPIHT algorithm, compression errors between the cube that is used as an input to the encoder and the decompressed cube output by the decoder are calculated in the interferogram domain, the spectral radiance domain, and the temperature and water vapor retrieval domains. In the descriptions that follow we refer to the cube input to the encoder as the "cube under test," the cube output from the decoder as the "decoded cube," and the original noise-free cube as the "noise-free cube." The cube under test and the noise-free cube differ only in that the cube under test includes simulated instrument noise.

Four error measures are reported in the interferogram domain: the mean-absolute-error (MA), the mean-squared-error (MSE), the maximum-absolute-error (MaxA), and the peak-signal-to-noise-ratio (PSNR). Let $x(i,j,k)$ be a sample from the cube under test, $x_{dec}(i,j,k)$ be a sample from the decoded cube and N be the total number of samples in the cube. The four errors above are calculated as

$$\mathrm{MA} = \frac{1}{N}\sum_{i,j,k}|x(i,j,k) - x_{dec}(i,j,k)| \tag{1}$$

$$\mathrm{MSE} = \frac{1}{N}\sum_{i,j,k}[x(i,j,k) - x_{dec}(i,j,k)]^2 \tag{2}$$

$$\mathrm{MaxA} = \max_{(i,j,k)}|x(i,j,k) - x_{dec}(i,j,k)| \tag{3}$$

$$\mathrm{PSNR} = 10\log_{10}\left(\frac{2^{16}-1}{\mathrm{MSE}}\right) \tag{4}$$

The units for MA and MaxA are digital counts (cnts), the units for MSE are digital counts squared (cnts^2), and the units for PSNR are dB. In the interferogram domain the same four errors are also calculated between the decoded cube and the noise-free cube.

The error measure used in the spectral radiance domain is the spectral RMS error which is computed as follows. The interferograms from 1024 equally spaced pixels in both the cube under test and the decoded cube are converted to the spectral radiance domain using a calibration equation very similar to one used by Best et al.[13] Converting the raw interferograms to spectral radiance measurements involves appodizing the interferograms prior to Fourier transformation (using a Kaiser-Bessel #6 function), correcting for instrument self emissions, applying the instrument spectral radiance responsivity, and correcting for the wavenumber shift in off-axis detectors. Appodization is used because the retrieval was trained with appodized spectra. The RMS error between the spectral radiances in the cube under test and the decoded cube is computed for each spectral bin. The units of the spectral RMS error are $\mathrm{mW/(m^2{\cdot}sr{\cdot}cm^{-1})}$.

The retrieval domain errors are computed from the subset of the 1024 pixels used for spectral domain errors that are classified as clear. Only clear pixels are used because retrievals on cloudy pixels can not be accurately computed with the retrieval used here unless cloud amount, height, and opacity are all known; or a "clear-column radiance" estimate is computed.[14] Pixels were classified as clear if the brightness temperature in the 893.5–903.780 $\mathrm{cm^{-1}}$ window exceeded a threshold of 272 K for Cube 2 and 294 K for Cube 5. This window brightness temperature criteria is one of three used by Zhou et al.[15] to classify pixels as clear.

Temperature and water vapor retrievals are performed on the subset of clear pixels in both the cube under test and the decoded cube using University of Wisconsin-Madison statistical retrieval prototype algorithms. The retrieval prototype algorithms are essentially an implementation of the theory presented by Huang and Antonelli[16] using 9,000 global radiosonde profiles and corresponding simulated top-of-the-atmosphere spectral radiances as the training set. Both the LWIR and SMWIR bands are used to produce a retrieval for a given cube. The RMS error between the retrieved profiles in the cube under test and the decoded cube are computed at each atmospheric pressure level. The error measure used in the temperature retrieval domain is the profile RMS error with units of Kelvin. The error measure for the water vapor retrieval domain is the profile RMS percentage error.

5. EXPERIMENTAL RESULTS

Table 1 shows the results in the interferogram domain at the three different nominal bit rates, with errors calculated between the cube under test and the decoded cube. The values in the Nominal Rate column are not actual bit rates. The actual bit rates are given in the legends in the spectral domain figures to follow. The errors in the MA and MSE columns indicate extremely high performance in the interferogram domain, with average compression errors of less than one least-significant-bit (LSB) for the LWIR cubes and just over one LSB for the SMWIR cubes. The absolute worst case errors in the cube for each test, shown in the MaxA column, also indicate excellent performance.

Table 2 gives the interferogram domain compression errors referenced to the noise-free cubes. As opposed to Table 1, when the errors are referenced to the noise-free cubes the PSNR increases as compression ratio increases, indicating that at the bit rates tested the compression process is removing more instrument noise than signal.

In the spectral domain it is useful to compare the compression errors with the magnitude of the simulated instrument noise. The simulated instrument noise used in this study is characterized in the spectral radiance domain by computing the spectral RMS error between the cubes under test and the noise-free cubes in the same manner used to compute compression errors. The only difference between these cubes is due to the simulated instrument noise. The results are shown in Fig. 6.

Fig. 7 shows the compression errors in the spectral radiance domain at three different bit rates. The actual bit rates are shown in the legends of each sub-figure. This figure shows that even at bit rates as low as 1.0–1.2 bpp the level of noise introduced by compression is comparable to the simulated instrument noise shown in Fig. 6.

Next we evaluate the compression errors in the retrieval domain. This should be viewed as an indicator only since the prototype retrievals were not optimized for the GIFTS data used in these simulations. Fig. 8 shows the retrieval errors between the cube under test and the noise-free cube. These results show for the levels of spectral domain instrument noise given in Fig.6 the prototype retrieval yields RMS temperature errors between 0.3 and 0.8 K, and RMS water vapor percentage errors in the range from a few percent up to 20–30%.

Table 1. Interferogram Domain Compression Errors for the GIFTS-SPIHT Algorithm

	LWIR Complex Cube 2				LWIR Complex Cube 5			
Nominal Rate (bpp)	MaxA (cnts)	MA (cnts)	MSE ($cnts^2$)	PSNR (dB)	MaxA (cnts)	MA (cnts)	MSE ($cnts^2$)	PSNR (dB)
1.00	8	0.59	0.73	97.67	15	0.70	0.99	96.37
1.50	8	0.48	0.54	99.02	12	0.57	0.70	97.88
2.00	8	0.36	0.38	100.52	12	0.45	0.50	99.34
	SMWIR Complex Cube 2				SMWIR Complex Cube 5			
Nominal Rate (bpp)	MaxA (cnts)	MA (cnts)	MSE ($cnts^2$)	PSNR (dB)	MaxA (cnts)	MA (cnts)	MSE ($cnts^2$)	PSNR (dB)
1.00	12	1.53	3.90	90.42	19	1.62	4.38	89.92
1.50	10	1.25	2.66	92.08	12	1.33	3.00	91.56
2.00	8	0.99	1.74	93.92	9	1.06	1.96	93.40

Table 2. Interferogram Domain Compression Errors for the GIFTS-SPIHT Algorithm Referenced to Original Noise-Free Complex Cubes

	LWIR Complex Cube 2				LWIR Complex Cube 5			
Nominal Rate (bpp)	MaxA (cnts)	MA (cnts)	MSE ($cnts^2$)	PSNR (dB)	MaxA (cnts)	MA (cnts)	MSE ($cnts^2$)	PSNR (dB)
1.00	9	0.56	0.76	97.49	17	0.57	0.82	97.22
1.50	9	0.66	0.94	96.62	13	0.63	0.90	96.77
2.00	9	0.73	1.05	96.10	13	0.70	1.02	96.24
	SMWIR Complex Cube 2				SMWIR Complex Cube 5			
Nominal Rate (bpp)	MaxA (cnts)	MA (cnts)	MSE ($cnts^2$)	PSNR (dB)	MaxA (cnts)	MA (cnts)	MSE ($cnts^2$)	PSNR (dB)
1.00	19	1.46	4.36	89.93	20	1.45	4.32	89.98
1.50	19	1.74	5.60	88.85	20	1.71	5.51	88.92
2.00	18	1.90	6.30	88.33	17	1.88	6.27	88.36

Fig. 9 shows the compression errors in the temperature and water vapor retrieval domains. Since both LWIR and SMWIR cubes are required to perform the retrievals, the bit rates in these figures are calculated by dividing the total number of encoded bits from both LWIR and SMWIR cubes by the combined number of samples in the LWIR and SMWIR cubes. For Cube 2, at an average bit rate of 1.08 bpp (compression ratio of 14.8:1) the maximum temperature profile error is approximately 0.7 K, and for Cube 5 it is approximately 0.9 K at a 14.7:1 compression ratio. With the exception of one pressure level in Cube 2, the maximum RMS water vapor errors are close to 10% for both Cubes 2 and 5 at compression ratios of 14.8:1 and 14.7:1, respectively. The goal for GIFTS temperature and water vapor retrieval accuracies is 1 K and 15%, respectively, for 1 km to 2 km layers.[1,2] The results in Fig. 9 indicate that a high performance algorithm and an optimized retrieval would allow image-compressed data to meet GIFTS retrieval performance goals at compression ratios approaching 15:1.

6. CONCLUSIONS

The GIFTS-SPIHT algorithm serves as a benchmark for high performance image compression algorithms applied to the frames of imaging FTS datacubes. This algorithm was shown to yield spectral domain compression errors on the order of the simulated instrument noise and retrieval domain compression errors on the order of the goals for GIFTS retrieval accuracies, at bit rates as low as 1.0–1.2 bpp. We thus conclude that, algorithms employing high performance image compression techniques, such as SPIHT or JPEG2000,[17,18] have a high probability of providing the quality of data required by the scientific community, and should be considered as options for future applications similar to GIFTS when bandwidth is limited. A major advantage of such algorithms is minimal on-board storage requirements since only one frame must be buffered for each FPA before compression. Also, it

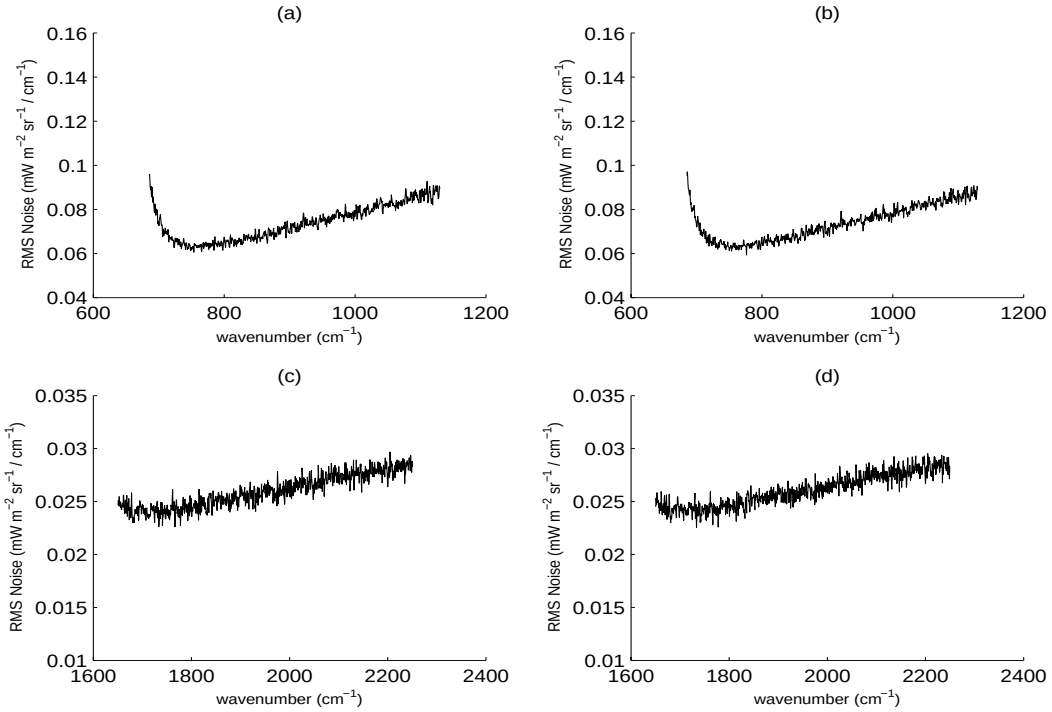

Figure 6. Simulated instrument noise in the spectral radiance domain: (a) LWIR Complex Cube 2, (b) LWIR Complex Cube 5, (c) SMWIR Complex Cube 2, (d) SMWIR Complex Cube 5.

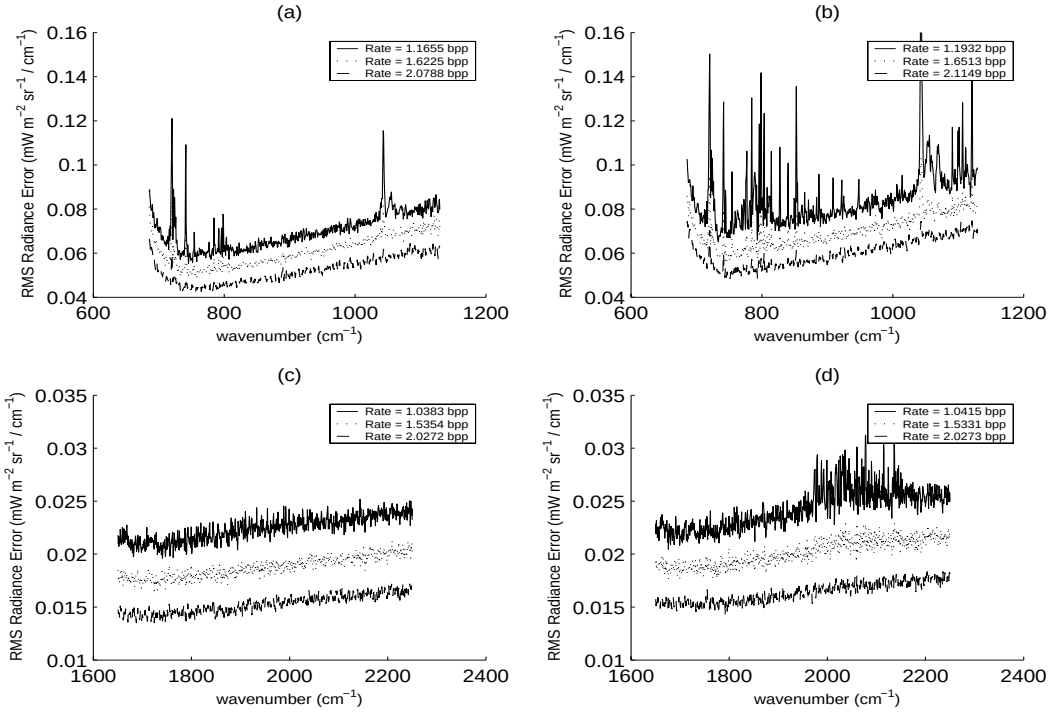

Figure 7. Spectral domain compression errors for the GIFTS-SPIHT algorithm: (a) LWIR Complex Cube 2, (b) LWIR Complex Cube 5, (c) SMWIR Complex Cube 2, (d) SMWIR Complex Cube 5.

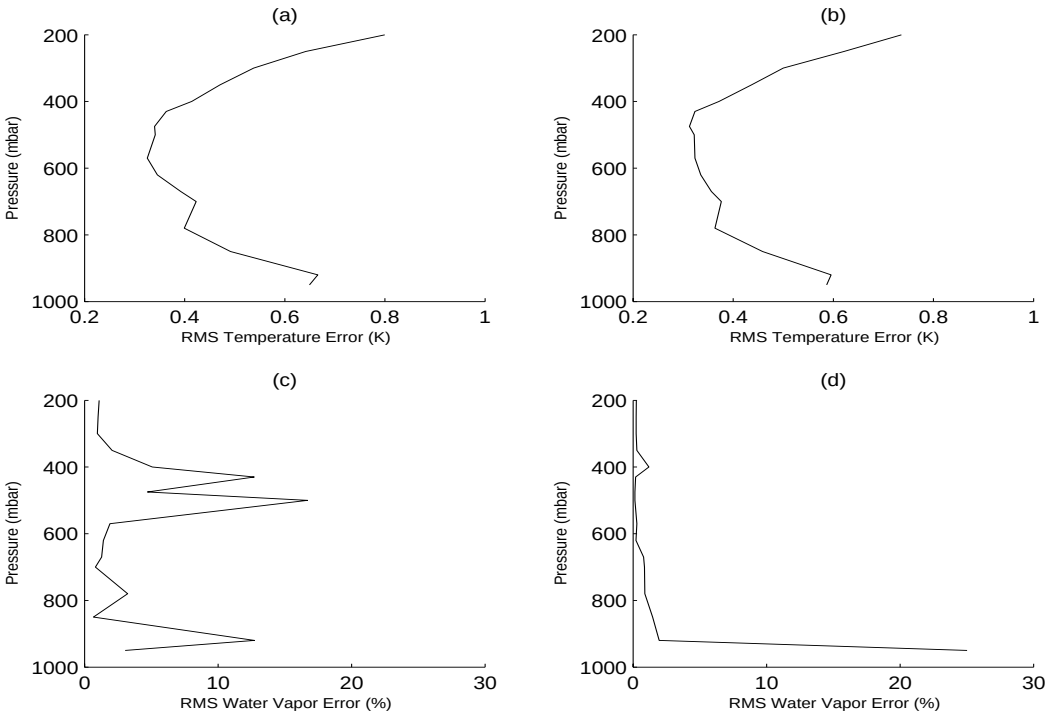

Figure 8. RMS retrieval errors between cubes with and without simulated instrument noise: (a) Complex Cube 2 temperature, (b) Complex Cube 5 temperature, (c) Complex Cube 2 water vapor, (d) Complex Cube 5 water vapor.

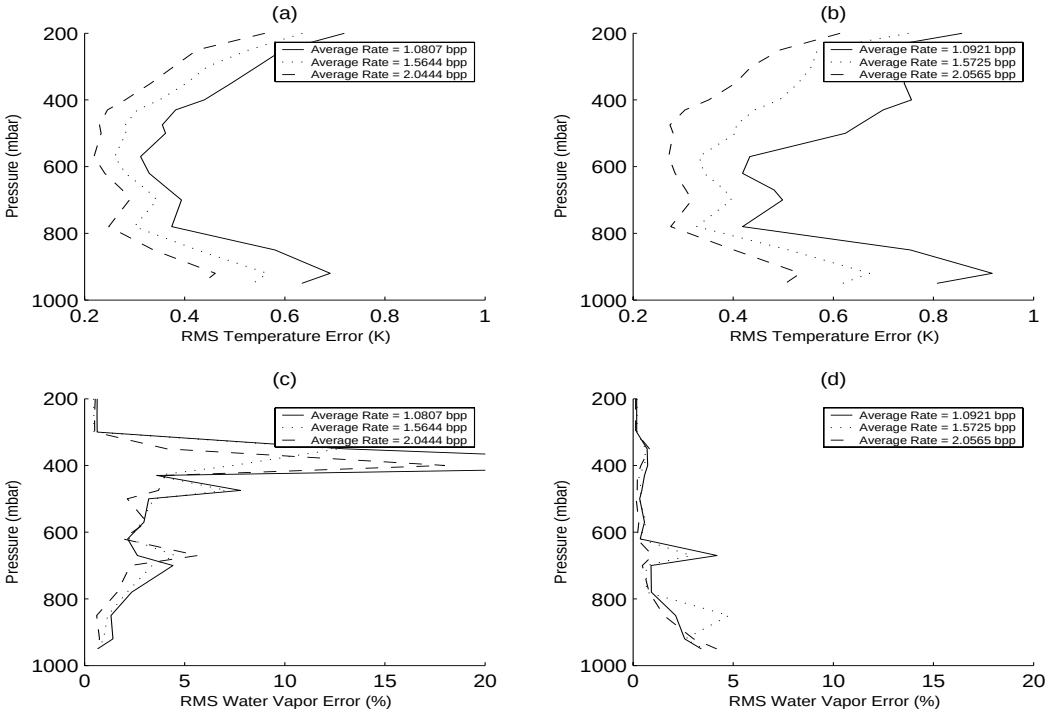

Figure 9. Retrieval domain compression errors for the GIFTS-SPIHT algorithm: (a) Complex Cube 2 temperature, (b) Complex Cube 5 temperature, (c) Complex Cube 2 water vapor, (d) Complex Cube 5 water vapor.

is likely that in the not too distant future, radiation hardened commercial off-the-shelf chips that implement the JPEG2000 standard will be available.

ACKNOWLEDGMENTS

Part of this work was performed under NASA contract NAS1-00071, University of Wisconsin contract G065726, and NOAA contracts 50-SPNA-1-00037 and 50-SPNA-8-00028. The authors gratefully acknowledge the University of Wisconsin at Madison for providing the synthetic GIFTS datacubes and prototype retrieval algorithms used in this research. Jason A. Swasey at the Space Dynamics Laboratory is acknowledged for contributions to the development of the tools used to measure compression performance.

REFERENCES

1. "Geostationary Imaging Fourier Transform Spectrometer (GIFTS) Concept Study Report." Submitted by NASA Langley Research Center to NASA Jet Propulsion Laboratory New Millennium Program Manager in response to NASA Research Announcement 98-OES-12, 1999.
2. W. L. Smith, F. W. Harrison, D. E. Hinton, H. E. Revercomb, G. E. Bingham, R. Petersen, and J. C. Dodge, "GIFTS – The precursor geostationary satellite component of the future earth observing system," in *IGARSS 2002 : remote sensing, integrating our view of the planet : 2002 IEEE International Geoscience and Remote Sensing Symposium : 24th Canadian Symposium on Remote Sensing*, pp. 357–361, Institute of Electrical and Electronics Engineers, (New York), 2002.
3. A. Thurgood, "GIFTS Sensor Module (SM) Overview," Tech. Rep. SDL/02-159, Space Dynamics Laboratory. (Presentation 13c at GIFTS-IOMI Preliminary Design Review given March 21, 2001).
4. F. L. Pedrotti and L. S. Pedrotti, *Introduction to Optics*, pp. 536–537. Prentice Hall, Englewood Cliffs, NJ, 2 ed., 1993.
5. H.-L. Huang, H. E. Revercomb, J. Thom, P. B. Antonelli, B. Osborne, D. Tobin, R. Knuteson, R. Garcia, S. Dutcher, J. Li, and W. L. Smith, "Geostationary imaging FTS (GIFTS) data processing: Measurement simulation and compression," in *Proc. SPIE*, **4151**, pp. 103–114, 2000.
6. "Simulated compression algorithm dataset description document," Tech. Rep. UW-GIFTS-04-007, University of Wisconsin-Madison Space Science and Engineering Center, Aug. 2000.
7. "Signal and noise relationships for GIFTS simulated data cubes," Tech. Rep. UW Technical Note 07-001, Draft, University of Wisconsin-Madison Space Science and Engineering Center, Jan. 2001.
8. F. L. Pedrotti and L. S. Pedrotti, *Introduction to Optics*, pp. 225–228. Prentice Hall, Englewood Cliffs, NJ, 2 ed., 1993.
9. A. Said and W. A. Pearlman, "A new, fast, and efficient image codec based on set partitioning in hierarchical trees," *IEEE Trans. on Circuits and Systems for Video Technology* **6**, pp. 243–249, June 1996.
10. M. Antonini, M. Barlaud, P. Mathieu, and I. Daubechies, "Image coding using wavelet transform," *IEEE Trans. on Image Processing* **1**, pp. 205–220, Apr. 1992.
11. C. M. Brislawn, "Classification of nonexpansive symmetric extension transforms for multirate filter banks," *Applied and Computational Harmonic Analysis* **3**, pp. 337–357, 1996.
12. G. W. Cantwell, "Data compression algorithms for the Geosynchronous Imaging Fourier Transform Spectrometer," Master's thesis, Utah State University, Logan, UT, 2003.
13. F. A. Best, H. E. Revercomb, G. E. Bingham, R. O. Knuteson, D. C. Tobin, D. D. LaPorte, and W. L. Smith, "Calibration of the geostationary imaging fourier transform spectrometer (GIFTS)," in *Proc. SPIE*, **4151**, pp. 21–31, 2000.
14. W. L. Smith, "An improved method for calculating tropospheric temperature and moisture from satellite radiometer measurements," *Monthly Weather Review* **96**(6), pp. 387–396, 1968.
15. D. K. Zhou, W. L. Smith, J. Li, H. B. Howell, G. W. Cantwell, A. M. Larar, R. O. Knuteson, D. C. Tobin, H. E. Revercomb, and S. A. Mango, "Thermodynamic product retrieval methodology and validation for NAST-I ," *Applied Optics* **41**, pp. 6957–6967, 2002.
16. H.-L. Huang and P. Antonelli, "Application of principal component analysis to high resolution infrared measurement compression and retrieval," *Journal of Applied Meteorology* **40**, pp. 365–388, Mar. 2001.

17. C. Christopoulos, A. Skodras, and T. Ebrahimi, "The JPEG2000 still image coding system: An overview," *IEEE Trans. on Consumer Electronics* **46**, pp. 1103–1127, Nov. 2000.
18. ISO/IEC JTC 1/SC 29/ WG 1, "ISO/IEC FCD 15444-1: JPEG 2000 Part I Final Committee Draft Version 1.0." [http://www.jpeg.org/FCD15444-1.pdf], Mar. 1996.